Bioorganic & Medicinal Chemistry Letters 21 (2011) 1134–1140

Contents lists available at ScienceDirect

Bioorganic & Medicinal Chemistry Letters

journal homepage: www.elsevier.com/locate/bmcl

Optimization of a novel class of benzimidazole-based farnesoid X receptor (FXR) agonists to improve physicochemical and ADME properties

Hans G. F. Richter [a,*], G. M. Benson [a], K. H. Bleicher [a], D. Blum [a], E. Chaput [a], N. Clemann [a], S. Feng [b], C. Gardes [a], U. Grether [a], P. Hartman [a], B. Kuhn [a], R. E. Martin [a], J.-M. Plancher [a], M. G. Rudolph [a], F. Schuler [a], S. Taylor [a]

[a] F. Hoffmann-La Roche Ltd, Pharmaceutical Research, Grenzacherstrasse, CH-4070 Basel, Switzerland
[b] Roche R&D Center (China) Ltd, 720 Cai Lun Road, Building 5, Pudong, Shanghai 201203, China

ARTICLE INFO

Article history:
Received 9 November 2010
Revised 22 December 2010
Accepted 23 December 2010
Available online 31 December 2010

Keywords:
Farnesoid X receptor agonist
FXR
Nuclear receptor
Lead optimization
ADME
X-ray structure

ABSTRACT

Structure-guided lead optimization of recently described benzimidazolyl acetamides addressed the key liabilities of the previous lead compound **1**. These efforts culminated in the discovery of 4-{(*S*)-2-[2-(4-chloro-phenyl)-5,6-difluoro-benzoimidazol-1-yl]-2-cyclohexyl-acetylamino}-3-fluoro-benzoic acid **7g**, a highly potent and selective FXR agonist with excellent physicochemical and ADME properties and potent lipid lowering activity after oral administration to LDL receptor deficient mice.

The farnesoid X receptor (FXR, NR1H4) is a ligand-activated transcription factor and member of the nuclear hormone receptor superfamily. Cloned in 1995[1] and de-orphanized in 1999,[2] FXR has been identified as a key sensor for bile acids, with chenodeoxycholic acid (CDCA, Fig. 1) being the most effective endogenous activator.

Consistent with its function in regulating bile acid synthesis and profile, FXR is mainly expressed in organs that are involved in the enterohepatic circulation of bile acids that is, liver and intestine as well as kidneys and adrenal glands.[3] Upon activation of FXR by bile acids it represses the expression of CYP7A1 and CYP8B1, the rate-limiting enzyme of bile acid synthesis from cholesterol and of bile acid hydrophilicity, respectively, by increasing the expression of the atypical nuclear receptor small heterodimer partner (SHP). SHP then decreases the pro-transcriptional regulation of these genes by a third nuclear receptor liver receptor homologue 1 (LRH-1). FXR also controls enterohepatic circulation of bile acids by regulating the expression of bile acid transporters and binding proteins such as BSEP, IBABP, and NTCP.[4]

The combined effects of FXR agonism on bile acid composition and pool size is a decrease in the intestinal absorption of dietary lipids resulting in a reduction of plasma cholesterol and triglycerides. Besides its central role in the maintenance of bile acid homeostasis, FXR also regulates genes affecting triglyceride metabolism (e.g., apoCII, apoCIII, SREBP1-1c)[5] leading to reduced plasma triglyceride levels. FXR is also involved in glucose homeostasis. In various mouse models[6] FXR agonists were shown to decrease plasma glucose levels through the modulation of different target genes involved in the regulation of hepatic gluconeogenesis (e.g., PEPCK or G6Pase) and glycogen synthesis (e.g., phosphorylation of GSK3β), respectively. In addition, FXR was shown to improve insulin sensitivity, although the underlying molecular mechanisms and the contribution of FXR-independent pathways still need to be determined. Consistent with these mechanisms and with positive results from pre-clinical animal studies, FXR modulators have a great therapeutic potential in the treatment of dyslipidemia, atherosclerosis and diabetes. Further studies also suggest a possible role for FXR agonists in treating cholestasis,[7] gallstone disease,[8] nonalcoholic steatohepatitis (NASH)[9] and diabetic nephropathy,[10] although the final proof in humans is still to be established.

Since the deorphanization of FXR several potent steroidal and non-steroidal FXR agonists have been reported (Fig. 1). GW4064,[11] the first high-affinity non-steroidal ligand, and later Fexaramine,[12] served as useful tool compounds to investigate the FXR pharmacology and to elucidate the topology and active conformation of the FXR binding site. However, sub-optimal in vitro and

* Corresponding author. Tel.: +41 61 688 1330; fax: +41 61 688 6459.
E-mail address: hans.richter@roche.com (H.G.F. Richter).

0960-894X/$ - see front matter © 2011 Elsevier Ltd. All rights reserved.
doi:10.1016/j.bmcl.2010.12.123

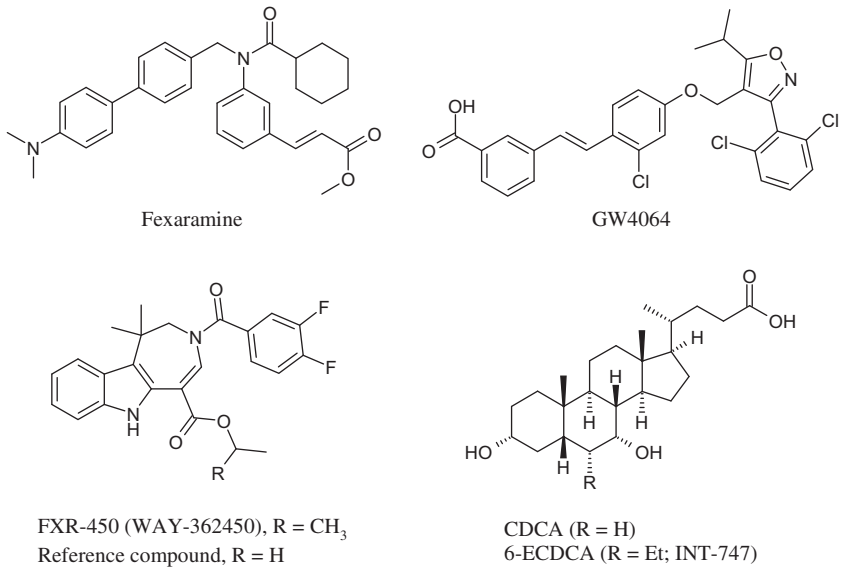

Figure 1. Representative FXR agonists.

in vivo characteristics, such as poor rat pharmacokinetic properties or instability under UV light and the presence of a potentially toxic stilbene moiety in the case of GW4064, precluded further development of these compounds.[13] Researchers from Wyeth and Exelixis published the synthesis of the non-steroidal agonist FXR-450 that recently entered clinical trials.[14] A follow-up paper described the approaches applied for improving the physicochemical properties of FXR-450.[15] The most advanced FXR agonist to date is the semi-synthetic bile acid derivative 6-ECDCA (a mixed FXR/GPBAR1 agonist)[16] which recently completed Phase II clinical trials in patients with primary biliary cirrhosis.[17]

We recently reported on the synthesis and structure–activity relationship (SAR) profiling of a novel class of potent and selective benzimidazole-based FXR agonists as exemplified by our lead structure **1** (Fig. 2).[18] Although **1**, a potent, partial agonist at the FXR receptor is endowed with oral activity in an in vivo model of dyslipidemia, it was found to have poor physicochemical properties such as high lipophilicity and poor aqueous solubility. Surprisingly, the compound also inhibited the hERG potassium channel in vitro with an IC_{50} of 1.6 μM.

Our lead optimization efforts, therefore, concentrated on the introduction of polarity to reduce the high lipophilicity and increase solubility and bioavailability (mouse $F = 1.7\%$) and to overcome the hERG liability of **1**.

In accordance with the hydrophobic nature of the ligand binding site of human FXR, the original SAR[18] indicated little scope for the introducing polarity into these novel agonists. However, following further analysis of structural information generated in-house, we identified a more polar, as yet unexplored region in FXR consisting of Gln267, Asn297, His298, Arg335 and three water molecules in the proximity of the amide-bound cyclohexyl group (Fig. 3). Comparison with a published co-crystal structures of rat

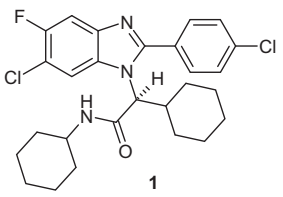

Figure 2. Lead compound from the benzimidazolyl acetamide class.

FXR with 6-ECDCA revealed that the carboxylate of 6-ECDCA is located in this region and interacts through charge-assisted hydrogen bonds with the corresponding rat Arg328.[19] We therefore initiated a structure-guided design program in which we investigated a variety of polarity-conferring substituents at different distances from and orientation to the amide group, targeting in particular an electrostatic interaction with Arg335.

Two strategies were followed for the synthesis of the novel benzimidazoles. For both, single enantiomers were obtained by chiral chromatography. The assignment of the absolute stereochemistry was based on several co-crystal structures (incl. crystallizations with racemates in which only the *S* enantiomers bound) as well as small molecule X-ray crystallography of

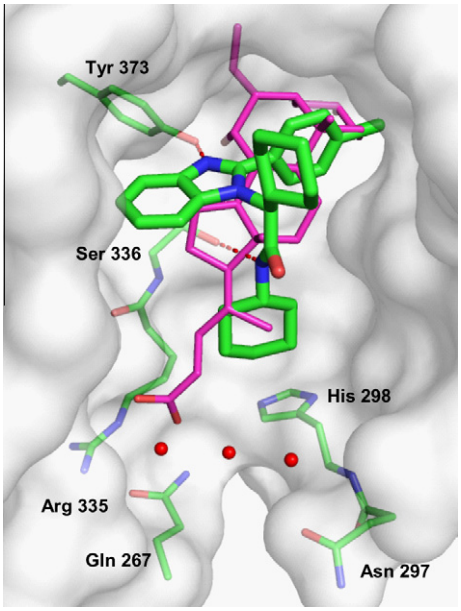

Figure 3. X-ray structure of the 5,6-di-H analogue[18] of benzimidazolyl acetamide **1** bound to human FXR (PDB: 3OKI) illustrating the targeted polar binding site region. The front of the FXR binding site is removed for clarity. Protein–ligand hydrogen bonds to Ser336 and Tyr373 are depicted as red dashed lines. The structure is overlaid with the 6-ECDCA/rat FXR complex (magenta, PDB: 1ot7, protein not shown).

Table 1
Binding and functional activity at human FXR for selected benzimidazolyl acetamides

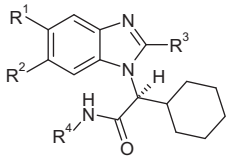

Compound	R^1, R^2	R^3	R^4	IC_{50}[a] (μM)	EC_{50} (μM) (efficacy)[b]
		GW4064 (see Fig. 1)		0.112	0.91 (99%)
		Reference compound (see Fig. 1)		0.021	0.085 (39%)
1	F, Cl	4-Cl-Ph	C_6H_{11}	0.013	0.1 (42%)
7a	F, F	4-Cl-Ph	C_6H_{11}	0.010	0.05 (31%)
7b	F, F	4-Cl-Ph	*trans*-4-OH–C_6H_{10}	0.041	0.3 (40%)
7c	F, F	4-Cl-Ph	*trans*-4-CO_2H-C_6H_{10}	0.61	2.7 (26%)
7d	F, F	4-Cl-Ph	4-CO_2H-Ph	0.05	2.5 (27%)
7e	F, F	4-Cl-Ph	2-CO_2H-Ph	0.32[c]	>40[c]
7f	F, F	4-Cl-Ph	3-CO_2H-Ph	1.3[c]	10.7 (14%)[c]
7g	F, F	4-Cl-Ph	2-F-4-CO_2H-Ph	0.037	0.3 (30%)
7h	F, F	4-Cl-Ph	2-Cl-4-CO_2H-Ph	0.009	0.3 (54%)
7i	F, F	4-Cl-Ph	2-Me-4-CO_2H-Ph	0.02	0.5 (51%)
7j	F, F	4-Cl-Ph	2-CF_3-4-CO_2H-Ph	0.008	0.05 (59%)
7k	F, F	4-Cl-Ph	2-MeO-4-CO_2H-Ph	0.74	10.4 (32%)
7l	F, F	4-Cl-Ph	2,6-F_2-4-CO_2H-Ph	0.004	1.4 (48%)
7m	F, F	4-Cl-Ph	4-CO_2H-CH_2-Ph	1.4[c]	4.9 (14%)[c]
7n	F, F	4-Cl-Ph	4-CO_2H-CH_2CH_2-Ph	0.06[c]	2.0 (18%)[c]
7o	F, F	4-Cl-Ph	2-F-4-CO_2H-CH_2CH_2-Ph	0.013	0.036 (17%)
7p	F, F	4-Cl-Ph	2-F-4-CO_2H-*Cc*-Pr-O-Ph	0.001	0.6 (21%)
7q	F, F	4-Cl-Ph	*trans*-4-CO_2H-C_6H_{10}-CH_2	3.9[c]	10.0 (16%)[c]
7r	F, F	4-Cl-Ph	*trans*-4-CO_2H-CH_2-C_6H_{10}	0.61	5.0 (27%)
7s	F, F	4-Cl-Ph	*trans*-4-CO_2H-CH_2O-C_6H_{10}	0.83	9.9 (26%)
7t	F, F	4-Cl-Ph	4-Me-5-CO_2H-thiazole	0.09[c]	10.4 (10%)[c]
7u	F, F	4-Cl-Ph	4-CF_3-5-CO_2H-thiazole	0.20[c]	>40[c]
7v	F, F	4-Cl-Ph	4-CO_2H-2-Py	0.20[c]	10.6 (20%)[c]
7w	F, F	4-Cl-Ph	4-CO_2H-3-Py	3.1[c]	>40[c]
7x	F, F	4-Cl-Ph	2-F-4-(1*H*-tetrazol-2-yl)-Ph	0.008	0.3 (21%)
7y	F, H	4-Cl-Ph	2-F-4-CO_2H-Ph	0.04	1.1 (25%)
7z	H, H	4-Cl-Ph	2-CF_3-4-CO_2H-Ph	0.01	0.09 (35%)
7aa	F, F	6-Cl-pyridin-3-yl	*trans*-4-CO_2H-C_6H_{10}	1.7	9.7 (18%)
7ab	F, F	2,6-$(MeO)_2$-pyridin-3-yl	*trans*-4-CO_2H-C_6H_{10}	0.21	1.7 (19%)
7ac	F, F	2-MeO-6-Cl-pyridin-3-yl	*trans*-4-CO_2H-C_6H_{10}	0.29	1.1 (21%)

[a] SPA scintillation proximity assay (SPA). Binding affinity was assessed in a radioligand displacement assay according to the method of Nichols, J. S. et al.[22] Values are means of at least two experiments.
[b] Transactivation assay. Transactivation activity was measured using a luciferase transcriptional reporter-gene assay according to the method of Jingami.[23] Efficacies are relative to GW4064 set at 100%.
[c] Value for racemic mixture.

compounds **7d** and **7g** that proved *S* configuration at the chiral center.[20]

The first synthetic route was based on a four-component Ugi reaction treating Boc-protected phenylene diamines with carboxylic acids, aldehydes and isonitriles as previously reported (**1**, **7a**, **7y**, **7aa**, **7ab**, **7ac**, Table 1).[18] Although this method gave us rapid access to the target molecules, the limited number of available isonitriles of interest triggered the development of an additional synthetic route as depicted in Scheme 1. This methodology was used preferably for the synthesis of 'symmetrical' benzimidazoles ($R^1 = R^2$ = F or H). Benzimidazole **2** was synthesized by condensation of commercially available 4,5-difluoro-benzene-1,2-diamine and 4-chloro-benzoic acid. Alkylation of **2** with α-bromo-cyclohexyl-acetic acid ester **3**, prepared in a three-step, one-pot procedure from commercially available cyclohexyl-acetic acid,[21] gave compound **4**. Cleavage of the ethyl ester in **4** provided the acid **5**. Amide coupling of **5** with different amines and anilines yielded amides **6**. Methyl or ethyl ester groups on substituent R^3 in intermediates **6** (either prepared via Ugi reaction or as described above) were cleaved under basic conditions to provide the racemic acids **7**. Analogue **7x** carrying a tetrazole-substituted R^3 was prepared by converting the cyano group in **6** using standard procedures. Analogue **7z** ($R^1 = R^2$ = H) was prepared using the same protocol, starting from commercially available 2-(4-chlorophenyl)benzimidazole.

The structure–activity relationship profile for the newly synthesized compounds is summarized in Table 1. Based on our previous SAR we chose the equipotent 6-fluoro analogue of **1 (7a)** to explore the amide exit vector. The binding affinity of the newly synthesized compounds was evaluated using a scintillation proximity assay (SPA).[22] Functional activity was determined in a Gal-4 transactivation assay[23] using the human FXR ligand binding domain (maximal efficacy relative to maximal efficacy of GW4064 in this assay). As with analogues of **1**,[18] the *R* enantiomers were shown to be significantly less potent agonists or else inactive (at concentrations up to 40 μM) versus the *S* enantiomers. Consequently, we first tested the racemate activity and, if this proved interesting, single enantiomers were prepared and tested.

Introduction of a hydroxy group in the 4-position of the amide-bound cyclohexyl ring in **7a** (**7b**) led to fourfold drop in binding affinity and potency while the efficacy was maintained. Replacing the hydroxy function in **7b** with a carboxylate group (**7c**) led to a

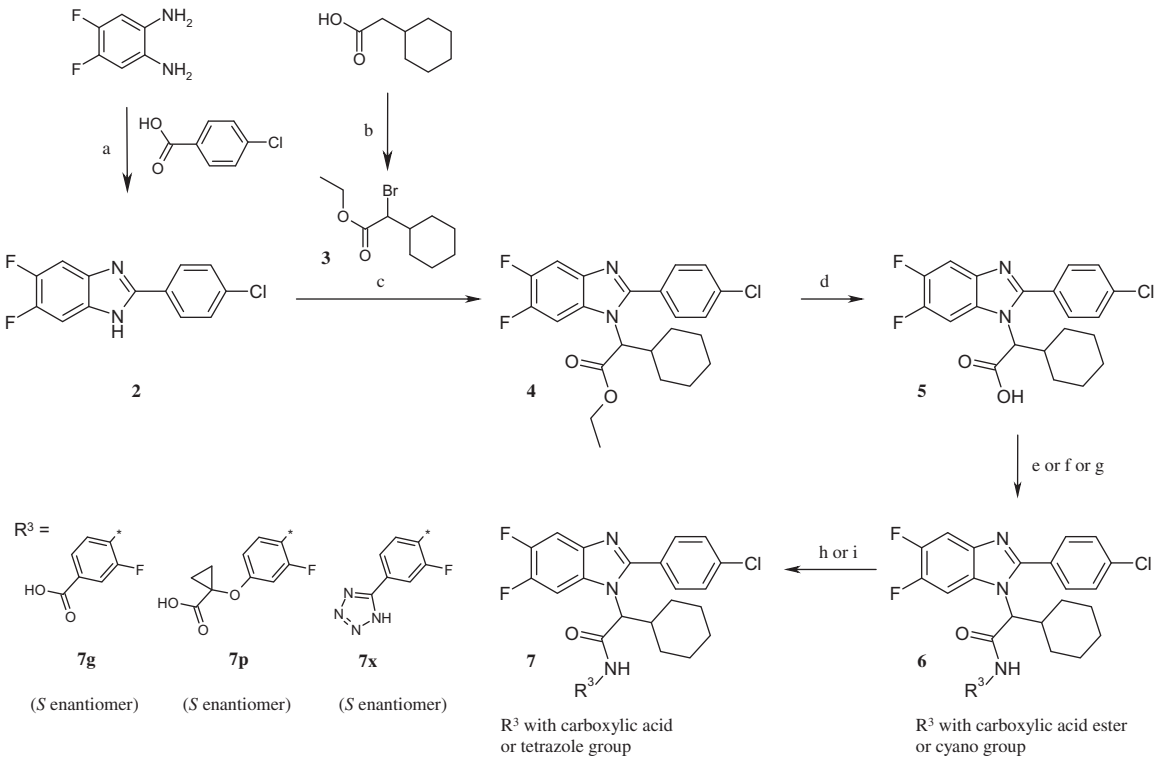

Scheme 1. Synthesis of novel benzimidazolyl acetamides. Reagents and conditions: (a) polyphosphoric acid, 160 °C (77%); (b) (i) $SOCl_2$, reflux; (ii) Br_2, reflux; (iii) EtOH, 0 °C to rt (99% crude over three-steps, one-pot); (c) **3** (3.75 equiv), Cs_2CO_3 (3.75 equiv), DMF, 100 °C (79%); (d) LiOH (3 equiv), dioxane, water, reflux (99%); (e) $SOCl_2$, reflux; then amine, pyridine (**7i**, **7j**, **7w**, 62–84%) or DMAP (**7d**, **7g**, **7h**, **7k**, **7l**, **7p**, **7s**, **7v**, **7x**, 47–97%) or Huenig's base (**7b** (66%), **7q** (67%)), CH_2Cl_2, 0 °C to rt; (f) HATU, Huenig's base, CH_2Cl_2, rt (**7c**, **7e**, **7f**, **7m**, **7n**, **7t**, **7u**, 17–82%); (g) 2-chloro-1-methylpyridium iodide, NEt_3, CH_2Cl_2, 40 °C (**7r**, 86%); (h) LiOH, dioxane, water, reflux (67–99%) or NaOH, acetonitrile, water, microwave, 100 °C (**7c**, 99%); (i) NaN_3, $HNEt_3Cl$, *o*-xylene, 145 °C (**7x**, 29%).

more pronounced loss in binding affinity and potency. Binding affinity was improved by exchanging the cyclohexyl with a phenyl ring (**7d**). These early results indicated that the chosen exit vector and receptor sub-pocket tolerates the introduction of polar groups. Moving the carboxylate group in **7d** to the 2- or 3-position (**7e**, **7f**) led to a loss in binding activity and an even more pronounced reduction of potency, with derivative **7e** failing to trigger a functional response. Acyclic aliphatic carboxylic acid residues $(CH_2)_nCO_2H$, $n = 1–5$ were significantly less active (data not shown). Substantially higher potency could be achieved by introducing fluoro, chloro, methyl or trifluoromethyl substituents in the 2-position of the 4-carboxy-substituted phenyl ring (**7g**–**7j**). For **7j** these effects are most pronounced with gains of binding affinity and potency of 7- and 49-fold, respectively.

Analysis of the structure of human FXR complexed with **7g** (Fig. 4) suggested additional beneficial contacts of the 2-substituent of the phenyl ring with two Met residues in a small hydrophobic sub-pocket as the main reason for the stronger interaction. It is also noteworthy that 2-substitution induces a change of the relative orientation of the phenyl and amide planes from in-plane (2-H, X-ray structure not shown) to orthogonal (2-des-H), resulting in different ring interactions. The perpendicular arrangement is also the preferred conformation of the amide-bound cyclohexyl ring (Fig. 3). The X-ray structure of **7g**[24] confirms that polar interactions are made between the newly introduced carboxylate group and its protein environment. Larger 2-substituents, for example, 2-methoxy (**7k**) again diminished binding affinity and potency, likely because the sub-pocket is too small. In contrast, introduction of a second fluoro substituent at the 2' position of **7g** (**7l**) was tolerated.

We found that the introduction of a methylene spacer between the phenyl ring and the carboxylate group significantly reduced the binding affinity (**7m**), whereas the longer ethylene spacer restored the binding affinity (**7n**). The activity of **7n** could again be improved through the introduction of a fluorine substituent in the 2-position (**7o**). By combining the 2-fluoro substituent with a

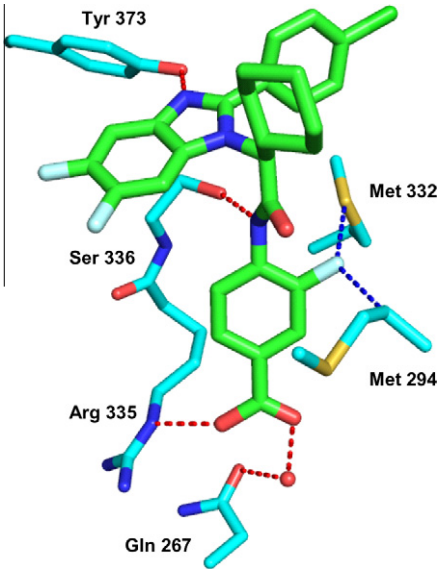

Figure 4. X-ray structure of benzimidazolyl acetamide **7g** bound to the ligand binding domain of human FXR (PDB: 3OMM. Resolution: 2.1 Å). Water-mediated and direct protein–ligand hydrogen bonds to Gln267, Arg335, Ser336 and Tyr373 (red, dashed lines) and hydrophobic interactions of the 2-F substituent to Met294 and Met332 (blue, dashed lines) are shown.

4-cyclopropoxy side-chain on the phenyl ring (**7p**) we identified the analogue with highest binding affinity in this series although this structural variation had little impact on potency as compared to **7g**. We also investigated the effects of additional methylene groups in the series of cyclohexyl analogues. Whereas the incorporation of a methylene (or a CH_2O) group between the cyclohexyl ring and the carboxylate group had only little effect on the binding affinity (**7r**, **7s** vs **7c**), moving the methylene spacer between the amide nitrogen and the cyclohexyl ring led to a drop of binding affinity and potency (**7q**). From a number of five-membered heterocycles investigated only compounds **7t** and **7u** showed sub-micromolar binding affinity, although functional activity was poor or even absent for **7t** and **7u**, respectively. Pyridine carboxylic acids (**7v**, **7w**) were also less active than the corresponding phenyl derivative **7d**. As a next step we investigated tetrazoles as bioisosteric replacements for the carboxylate group. As exemplified by **7x**, this change led to a fivefold improved binding affinity and comparable potency as for **7g**. In an attempt to reduce overall molecular weight and lipophilicity we also investigated the 6-des-fluoro and 5,6-des-fluoro substitution pattern on the benzimidazole core. As shown for **7y** and **7z**, this variation had little effect on the binding affinity and only a trend towards lower potency was observed compared to the 5,6-di-fluoro counterparts **7g** and **7j**, respectively. We finally investigated a number of pyridine substituents as less lipophilic replacements for the 4-chloro-phenyl substituent. Consistent with our previously generated SAR, unsubstituted pyridine substituents diminished the activity (data not shown). The 3-aza-analogue of **7c** (**7aa**) also showed weaker binding affinity and a significant drop in potency. However, appropriately substituted pyridines such as **7ab** and **7ac**, especially with a 2-methoxy substituent on the pyridine ring, showed a two to threefold increase in binding affinity with a trend to higher potency as compared to **7c**, underlining the broad scope for structural variation within this compound series also at this position.

Comparison of in vitro binding, potency and efficacy data with in vivo efficacy (plasma triglyceride and LDL cholesterol lowering in LDL receptor deficient mice) led us to identify binding IC_{50}s as the best predictor for in vivo activity provided that in vitro efficacy was $\geqslant$10% in the transactivation assay (results not shown). It is possible that differences in binding to cellular proteins and/or recruitment of co-activators or co-repressors to the artificial FXR/GAL4 complex within the nucleus could explain why in vitro activity and efficacy did not better predict in vivo efficacy.

Following the SAR assessment several compounds were selected for profiling of their physicochemical properties, in vitro metabolic stability, inhibition of three major human CYP isoforms, and potential to inhibit the potassium hERG channel. The results are summarized in Table 2. Whereas the introduction of a hydroxy group in **7a** (**7b**) slightly improved the solubility, lipophilicity stayed in a high range. As expected, analogues with a carboxylate or tetrazole moiety had significantly better aqueous solubility and much lower lipophilicity (log *D* 1.91–3.06).

The permeability of compounds **7d** and **7g** in an artificial permeation assay were evaluated and both samples showed a high permeability over the full pH range of 3.0–8.0. Based on similarity of physicochemical properties, permeability is expected to be high for the other compounds as well.

All of the compounds showed an improved CYP450 profile versus **7a** except for tetrazole **7x**, which was found to have a comparable profile to **7a** but inferior profile to its carboxylate counterpart **7h**, indicating low drug–drug interaction potential. Metabolic stability in mouse and human microsomes was greatly improved for all the tested compounds versus **7a**.

Finally, we tested the compounds for their hERG potassium channel inhibitory activity. Compared to **7a**, compounds **7b** and **7c** showed a fivefold reduced hERG activity, although moderate activity was retained (IC_{50} 7.3 μM and 7.6 μM, respectively). Compounds **7d**, **7g**, **7p**, and **7z** however showed substantially attenuated hERG affinity with IC_{50} values greater than 20 μM. Interestingly, we found that the introduction of a carboxyl group onto the phenyl ring was not sufficient to circumvent the hERG activity of the tested derivatives. By replacing the 2-fluoro substituent in **7g** by a chloro (**7h**) or a methyl group (**7i**) the compounds picked up hERG activity again with **7i** being the most potent compound in this series with an IC_{50} of 0.7 μM.

Selectivity of the compounds for FXR was evaluated using a panel of reporter-gene transcriptional assays for other nuclear receptors including PPAR-α, -δ, -γ, LXR-α, -β and RXR-α. No

Table 2
Solubility, lipophilicity, CYP450 inhibition, microsomal clearance and hERG inhibition data for selected benzimidazolyl acetamides

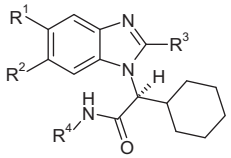

Compound	R^1, R^2	R^3	R^4	Solubility[a] (μg/mL)	log *D*[b]	CYP IC_{50} (μM) 3A4, 2D6, 2C9	Cl_{int} (h/m)[c] ((μL/min)/mg protein)	hERG IC_{50}[d] (μM)
1	F, Cl	4-Cl-Ph	C_6H_{11}	<1	>4	4.5, >50, >50	137/909	1.6
7a	F, F	4-Cl-Ph	C_6H_{11}	<1	>4	7.6, 32, 6.7	221/1654	1.4
7b	F, F	4-Cl-Ph	*trans*-4-OH-C_6H_{10}	17	>4	33, >50, 40	30/20	7.3
7c	F, F	4-Cl-Ph	*trans*-4-CO_2H-C_6H_{10}	395	2.49	>50, >50, >50	5/6	7.6
7d	F, F	4-Cl-Ph	4-CO_2H-Ph	88	3.06	37, >50, 32	8/19	>20
7g	F, F	4-Cl-Ph	2-F-4-CO_2H-Ph	115	2.66	39, >50, 14	9/13	>20
7h	F, F	4-Cl-Ph	2-Cl-4-CO_2H-Ph	51	2.98	23, >50, 18	31/26	7.8
7i	F, F	4-Cl-Ph	2-Me-4-CO_2H-Ph	32	2.83	>50, >50, 19	12/8	0.7
7p	F, F	4-Cl-Ph	2-F-4-CO_2H-Cc-Pr-O-Ph	280	2.32	>50, >50, 29	0/0	>20
7x	F, F	4-Cl-Ph	2-F-4-(1*H*-tetrazol-2-yl)-Ph	490	2.96	7.7, 31, 7.1	12/11	>10
7z	H, H	4-Cl-Ph	2-CF_3-4-CO_2H-Ph	175	2.34	49, 36, 28	12/21	>20
7ab	F, F	2,6-$(MeO)_2$-pyridin-3-yl	*trans*-4-CO_2H-C_6H_{10}	465	1.91	>50, >50, >50	1/17	>10
7ac	F, F	2-MeO-6-Cl-pyridin-3-yl	*trans*-4-CO_2H-C_6H_{10}	440	2.05	ND[e]	4/0	ND[e]

[a] Aqueous solubility at pH 6.5 in 0.05 M phosphate buffer.
[b] pH 7.4.
[c] Intrinsic clearance in human (h) and mouse (m) liver microsomes.
[d] Inhibition of hERG potassium channel determined by whole-cell patch-clamp experiments in a transfected CHO cell line.
[e] ND = not determined.

Table 3
Pharmacokinetic parameters of compound **7g** after intravenous and oral administration in male C57BL/6 mice and male Wistar rats[a]

Species	Dose (mg/kg)	Cl ((mL/min)/kg)	C_{max}/dose (ng/mL)	V_{ss} (L/kg)	AUC/dose (ng ∗ h/mL)	$t_{1/2}$ (h)	F (%)
Male C57BL/6 mouse[b]	4 (iv) 10 (po)	10.0	205.4	1.24	543.3	1.61	33%
Male Wistar rat[c]	2 (iv) 5 (po)	16.3	269.6	0.62	606.5	1.16	59%

[a] 7.5% gelatin in 0.62% aqueous NaCl and 30% *N*-methylpyrrolidinone in aqueous100 mM TRIS buffer pH 8.5 were used as vehicles for oral and intravenous administration, respectively.
[b] $n = 2$ per time point.
[c] $n = 3$ per time point.

cross-reactivity was observed with these receptors up to a concentration of 10 μM (data not shown).

The pharmacokinetic parameters of **7g** were determined in mice and rats and the data are summarized in Table 3. After oral dosing in mice the compound was characterized by a low clearance (Cl) of 10 mL/min/kg, moderate half-life ($t_{1/2}$) of 1.6 h, volume of distribution (V_{ss}) of 1.24 L/kg and moderate oral bioavailability (F) of 33% which resulted in an overall good exposure (AUC) of 5433 ng ∗ h/mL. In rats, **7g** had a slightly higher clearance of 16 mL/min/kg, a moderate half-life of 1.2 h, low volume of distribution of 0.62 L/kg and a good bioavailability of 59%, leading to a good exposure of 3033 ng ∗ h/mL.

Based on the high in vitro potency of **7g** for human FXR (Table 1) and murine FXR (IC_{50} 0.29 μM, EC_{50} 0.87 μM (38%)), selectivity and favorable pharmacokinetic properties we evaluated its effects on plasma lipid profiles in high-fat diet fed LDL receptor deficient ($LDLR^{-/-}$) mice.[25] $LDLR^{-/-}$ mice are reported to respond to FXR treatment with decreases in plasma cholesterol and triglycerides as a consequence of reduced intestinal absorption and decreased synthesis.[26] After five days of treatment (10 mg/kg po, QD), **7g** caused a statistically significant decrease in plasma total cholesterol (TC, −41%), low density lipoprotein cholesterol (LDL-C, −33%) and triglycerides (TG, −59%). These reductions were comparable to the effects seen with the reference compound (ethyl ester analogue of FXR-450, Scheme 1) dosed at 30 mg/kg/d (Fig. 5). PK monitoring of **7g** revealed a plasma exposure of 885 ng/mL (1.63 μM) after 2 h. This result further confirmed the improved pharmacokinetic properties of **7g** versus **1** (plasma exposure after 2 h of 0.95 μM at a dose of 30 mg/kg).[18]

In summary, we developed a novel class of potent and selective non-steroidal FXR agonists based on a benzimidazole acetamide scaffold. Our lead optimization efforts guided by structure-based drug design allowed us to address the key liabilities of the previous lead compound **1** through the identification of an exit vector which permitted the introduction of polar residues. Several compounds with a negatively charged functionality displayed excellent physicochemical, ADME and in vitro safety properties culminating in the discovery of 4-{(*S*)-2-[2-(4-chloro-phenyl)-5,6-difluoro-benzoimidazol-1-yl]-2-cyclohexyl-acetylamino}-3-fluoro-benzoic acid (**7g**) with favorable rodent pharmacokinetic properties and potent plasma lipid lowering effects in $LDLR^{-/-}$ mice after oral administration.

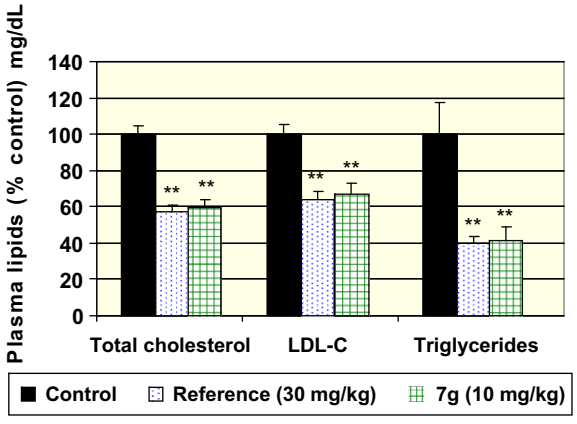

Figure 5. Effect of **7g** versus reference compound on plasma total cholesterol, LDL-C and triglycerides in $LDLR^{-/-}$ mice fed a high-fat diet for 15 days after 5 days oral treatment: (**) P <0.01 versus vehicle control, one way ANOVA followed by Dunnett's post hoc test.

Acknowledgement

The work of Martin Ritter and Kersten Klar is gratefully acknowledged.

References and notes

1. (a) Forman, B. M. et al *Cell* **1995**, *81*, 687; (b) Seol, W.; Choi, H.-S.; Moore, D. D. *Mol. Endocrinol.* **1995**, *9*, 72.
2. (a) Makishima, M.; Okamoto, A. Y.; Repa, J. J.; Tu, H.; Learned, R. M.; Luk, A.; Hull, M. V.; Lustig, K. D.; Mangelsdorf, D. J.; Shanz, B. *Science* **1999**, *284*, 1362; (b) Parks, D. J. et al *Science* **1999**, *284*, 1365; (c) Wang, H.; Chen, J.; Hollister, K.; Sowers, L. C.; Forman, B. M. *Mol. Cell* **1999**, *3*, 543.
3. Zhang, Y.; Kast-Woelbern, H. R.; Edwards, P. A. *J. Biol. Chem.* **2003**, *278*, 104.
4. Lee, F. Y.; Lee, H.; Hubbert, M. L.; Edwards, P. A.; Zhang, Y. *Trends Biochem. Sci.* **2006**, *31*, 572.
5. Zhang, Y.; Edwards, P. A. *FEBS Lett.* **2008**, *582*, 10.
6. (a) Zhang, Y.; Lee, F. Y.; Barrera, G.; Lee, H.; Vales, C.; Gonzalez, F. J.; Willson, T. M.; Edwards, P. A. *Proc. Natl. Acad. Sci. U.S.A.* **2006**, *103*, 1006; (b) van Dijk, T. H.; Grefhorst, A., et al *J. Biol. Chem.* **2006**, *281*, 11039; (c) Ma, K.; Saha, P. K.; Chan, L.; Moore, D. D. *J. Clin. Invest.* **2006**, *116*, 1102.
7. (a) Stedman, C.; Liddle, C.; Coulter, S.; Sonoda, J.; Alvarez, J. G.; Evans, R. M.; Downes, M. *Proc. Natl. Acad. Sci. U.S.A.* **2006**, *103*, 11323; (b) Jones, S. A. et al *J. Clin. Invest.* **2003**, *112*, 1678; (c) Fiorucci, S. et al *J. Pharmacol. Exp. Ther.* **2005**, *313*, 604.
8. (a) Doggrell, S. A. *Curr. Opin. Invest. Drugs* **2006**, *7*, 344; (b) Moschetta, A.; Bookout, A. L.; Mangelsdorf, D. J. *Nat. Med.* **2004**, *10*, 1235.
9. (a) Cariou, B. *Diabetes Metab.* **2008**, *34*, 685; (b) Kong, B.; Luyendyk, J. P.; Tawfik, O.; Guo, G. L. *J. Pharmacol. Exp. Ther.* **2009**, *328*, 116.
10. Levi, M. et al *Diabetes* **2007**, *56*, 2485.
11. Maloney, P. R. et al *J. Med. Chem.* **2000**, *43*, 2971.
12. Evans, R. M. et al *Mol. Cell* **2003**, *11*, 1079.
13. Navas, F., III et al *Bioorg. Med. Chem. Lett.* **2009**, *19*, 4733.
14. Flatt, B. et al *J. Med. Chem.* **2009**, *52*, 904.
15. Lundquist, J. T., IV; Harnish, D. C., et al *J. Med. Chem.* **2010**, *53*, 1774.
16. Pellicciari, R.; Fiorucci, S.; Camaioni, E.; Clerici, C.; Costantino, G.; Maloney, P. R.; Morelli, A.; Parks, D. J.; Willson, T. M. *J. Med. Chem.* **2002**, *45*, 3569.
17. Press release Intercept Pharmaceuticals; http://www.interceptpharma.com.
18. Bleicher, K. H. et al *Bioorg. Med. Chem. Lett.* **2011**, *21*, 191.
19. Mi, L.-Z.; Devarakonda, S.; Harp, J. M.; Han, Q.; Pellicciari, R.; Willson, T. M.; Khorasanizadeh, S.; Rastinejad, F. *Mol. Cell* **2003**, *11*, 1093.
20. Crystallographic data for structures **7d** and **7g** have been deposited at the Cambridge Crystallographic Data Centre under the deposition numbers CCDC 804960 (**7d**) and 804961 (**7g**), respectively. Copies of these data can be obtained free of charge via the Internet at www.ccdc.cam.ac.uk/conts/retrieving.html (or from the Cambridge Crystallographic Data Centre, 12 Union Road, Cambridge CB21EZ, UK; fax: +44 1223 336 033; or deposit@ccdc.cam.ac.uk).
21. Schwenk, E.; Papa, D. *J. Am. Chem. Soc.* **1948**, *70*, 3626.
22. (a) Nichols, J. S.; Parks, D. J.; Consler, T. G.; Blanchard, S. G. *Anal. Biochem.* **1998**, *257*, 112; (b) Nichols, J. S.; Parks, D. J.; Consler, T. G.; Blanchard, S. G. *Anal. Biochem.* **1998**, *263*, 126 (corrigendum).

23. Kanaya, E.; Shiraki, T.; Jingami, H. *Biochem. J.* **2004**, *382*, 913.
24. Coordinates and diffraction data of the FXR co-crystal structures of **7d**, **7g**, **7i** and **7l** have been deposited with the Protein Data Bank (www.pdb.org) under accession codes 3OOF, 3OMM, 3OLF and 3OOK, respectively.
25. Repa, J. J.; Turley, S. D.; Quan, G.; Dietschy, J. M. *J. Lipid Res.* **2005**, *46*, 779.
26. (a) Zhang, Y.; Yin, L.; Anderson, J.; Ma, H.; Gonzalez, F. J.; Willson, T. M.; Edwards, P. A. *J. Biol. Chem.* **2010**, *285*, 3035; (b) Mencarelli, A.; Fiorucci, S. *J. Cell. Mol. Med.* **2010**, *14*, 79.